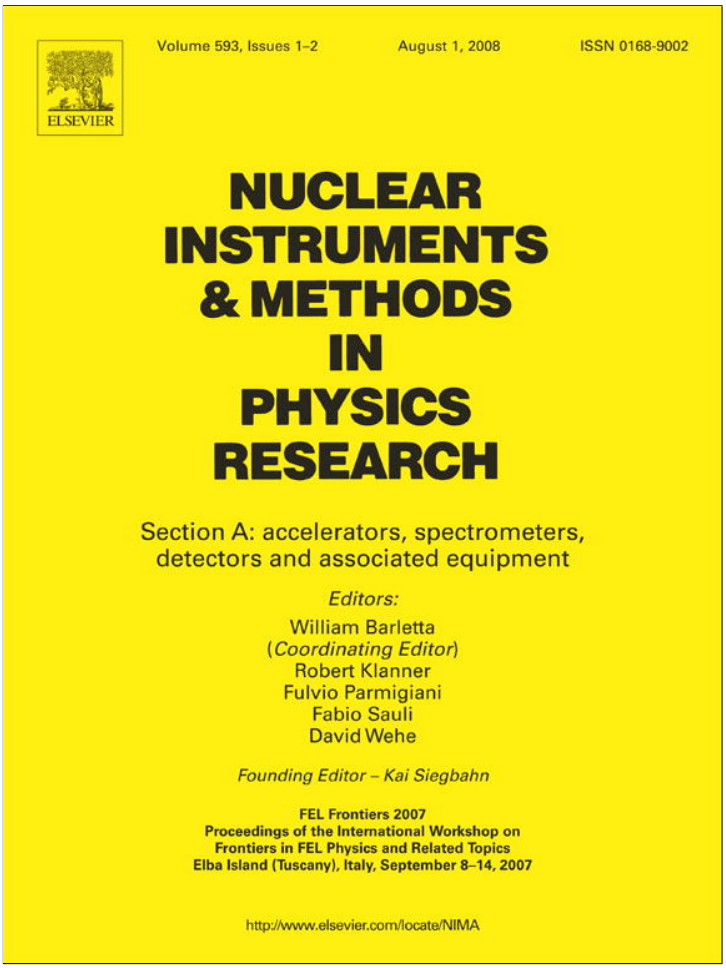

Nuclear Instruments and Methods in Physics Research A 593 (2008) 30–34

Contents lists available at ScienceDirect

Nuclear Instruments and Methods in Physics Research A

journal homepage: www.elsevier.com/locate/nima

Time-dependent FEL wavefront propagation calculations: Fourier optics approach

Oleg Chubar [a,*], Marie-Emmanuelle Couprie [a], Marie Labat [a,b], Guillaume Lambert [a,b], François Polack [a], Olivier Tcherbakoff [b]

[a] SOLEIL Synchrotron, L'Orme des Merisiers, Saint-Aubin BP 48, 91192 Gif-sur-Yvette, France
[b] CEA, DSM/SPAM, 91191 Gif-sur-Yvette, France

ARTICLE INFO

Available online 9 May 2008

Keywords:
Physical optics
Wavefront propagation
FEL
SASE

ABSTRACT

Numerical examples of time-dependent FEL wavefront propagation calculation and coherence analysis are presented. The calculations are performed using the Synchrotron Radiation Workshop (SRW)—wave-optics computer code optimized for synchrotron radiation, and the 3D FEL simulation code GENESIS 1.3. In the examples described, the electric field obtained at the exit of an FEL undulator after running GENESIS in time-dependent mode is transformed from time to frequency domain, and then propagated, using Fourier-optics methods implemented in SRW, through interferometer-type optical schemes. Time-averaged intensity patterns, obtained in image planes of the interferometers as a result of these simulations, allow for straightforward coherence characterization by visibility of interference fringes. The presented examples show that Fourier optics-based wavefront propagation method, as implemented in the SRW, can be effectively used for detailed analysis of characteristics of FEL radiation in time and in frequency domains. Besides, due to its high accuracy and CPU-efficiency, this method is very well suited for optimization of optical beamlines for fourth generation synchrotron radiation sources, for which accurate treatment of wave-optical phenomena, aimed to preserve radiation coherence and time structure, is of paramount importance.

1. Introduction

To fully exploit all great features of Synchrotron Radiation (SR) in the third and in the fourth generation sources [1,2], and to bring parameters of the sources to a good agreement with demands of users, high-accuracy simulation tools for the processes of the emission and wavefront propagation through optical beamlines are required. In the frame of classical electrodynamics, such simulation tools would operate with electric field of radiation or the entities directly derived from the field [3].

Two different physical-optics approaches to wavefront propagation simulations are currently popular: the approach based on asymptotic expansions[1] (its applications to SR and FEL wavefronts were described in the pioneering works [4,5]) and the Fourier optics [6] approach. This paper deals with the Fourier optics approach, as implemented in Synchrotron Radiation Workshop (SRW) [7,8].

From numerical point of view, the Fourier optics methods have a number of "strong points", e.g.:

- very high CPU efficiency[2];
- possibility to simulate multiple diffractive/refractive/reflective optical elements in "uniform" way without any increase of overall complexity[3];
- stability in case of "noisy" (not smooth or discontinuous) wavefronts[4];
- availability of large amount of data on electric field after a single propagation pass.

However, these methods have also "weak points", the most important of which is probably a relatively large amount of memory required by standard propagators.

* Corresponding author. Tel.: +33 1 6935 9841; fax: +33 1 6935 9451.
E-mail address: oleg.chubar@synchrotron-soleil.fr (O. Chubar).

[1] Mainly on the stationary phase method.

[2] Much superior to that of asymptotic expansions method.

[3] This is not the case for the asymptotic expansions method, which requires different types of expansions to be used for simulating optical aberrations and diffraction.

[4] For comparison, asymptotic expansion method is very sensitive to any lack of smoothness or to discontinuities of wavefronts and optical elements.

0168-9002/$ - see front matter © 2008 Elsevier B.V. All rights reserved.
doi:10.1016/j.nima.2008.04.058

While the Fourier optics methods are now routinely used for steady-state FEL wavefront propagation simulations [8,9], their application to time-dependent FEL wavefronts is still very limited, mainly because of the memory constraints. It should be mentioned that the pioneering work [5] also did not present extensive numerical examples that would illustrate time-dependent aspects of FEL wavefront propagation simulations.

On the other hand, one of the main trends for FEL developers is known to be creation of high-power diffraction- and Fourier-limited radiation pulses, which obviously require efficient techniques for combined "space–time" and "space–frequency" simulations and analysis.

Following this motivation, SRW code was modified to enable efficient "manipulations" (Fast Fourier Transforms (FFTs), resampling, resizing, …) not only with 2D (steady-state), but also with 3D (time- or frequency-dependent) wavefronts, with minimum of computational "overhead". Moreover, to facilitate data conversion at repetitive simulations, time-dependent FEL simulation code GENESIS 1.3 [10] has been integrated into SRW.

In the next sections, we briefly describe the computation method used by SRW, and present the results of propagation simulations of two types of FEL wavefronts through two different optical schemes. We have chosen the schemes that allow for analysis of spatial and temporal coherence of FEL radiation—the topics of high practical importance, which were addressed in a number of theoretical (e.g., Refs. [11,12]) and experimental (e.g., Refs. [13–15]) works.

2. Numerical method in brief

2.1. Time- and frequency-domain representations

Time- and frequency-domain complex electric fields $\vec{E}(\vec{r},t)$ and $\vec{E}(\vec{r},\omega)$ are well known to be related by the Fourier transform:

$$\vec{E}(\vec{r},\omega) = \int_{-\infty}^{\infty} \vec{E}(\vec{r},t)\,\exp(\mathrm{i}\omega t)\,\mathrm{d}t$$
$$\vec{E}(\vec{r},t) = \frac{1}{2\pi}\int_{-\infty}^{\infty} \vec{E}(\vec{r},\omega)\,\exp(-\mathrm{i}\omega t)\,\mathrm{d}\omega \qquad (1)$$

where t is time, ω is cyclic frequency, $\vec{r}$ is observation point.

While the electric field of initial FEL radiation is often calculated in time domain [10], its propagation in free space and through optical elements is usually treated in the frequency domain [16]. It is important therefore to use an efficient algorithm for Eq. (1). Such algorithm can be based on a prime-factor FFT, which would be applied "in place" to a complex electric field data structure, for many space points $\vec{r}$ in parallel.

2.2. Fourier-optics propagators

The propagation of transverse components of the frequency-domain electric field in free space is described by the Huygens–Fresnel principle, which, for small emission and observation angles, is [16]

$$\vec{E}_{\perp}(\vec{r}_2,\omega) \approx \frac{-\mathrm{i}\omega}{2\pi c}\iint_{\Sigma_1} \vec{E}_{\perp}(\vec{r}_1,\omega)\frac{\exp(\mathrm{i}\omega|\vec{r}_2-\vec{r}_1|/c)}{|\vec{r}_2-\vec{r}_1|}\mathrm{d}\Sigma_1 \qquad (2)$$

where the integration is performed over surface Σ_1; $\vec{r}_1$ is point on that surface (varying at the integration), $\vec{r}_2$ is an observation point, c is the speed of light. If Σ_1 is a plane, e.g., perpendicular to Z-axis, and $\vec{r}_2$ belongs to another plane, located at distance Δz from Σ_1, then $\mathrm{d}\Sigma_1 = \mathrm{d}x_1\mathrm{d}y_1$, $|\vec{r}_2-\vec{r}_1| = [\Delta z^2 + (x_2-x_1)^2 + (y_2-y_1)]^{1/2}$, and Eq. (2) is a convolution-type integral, which can be quickly calculated using 2D FFT.

In practice, direct application of the convolution theorem to Eq. (2) for the case of propagation between parallel planes may require very dense sampling of the electric field vs. transverse coordinates x_1 and y_1 (and/or x_2, y_2). However, if approximate values of wavefront radii and centers with respect to x_1 and y_1 are known, one can formally "subtract" the quadratic phase terms (mainly responsible for the phase growth) from a given wavefront; then, within the quadratic approximation for $|\vec{r}_2-\vec{r}_1|$, Eq. (2) can still be reduced to a convolution, with the necessity to re-scale the resulting wavefront, and to add a new (modified) quadratic phase term to it. This simple manipulation can dramatically reduce the amount of memory required for the propagation, while preserving high efficiency and accuracy of the Fourier optics method.

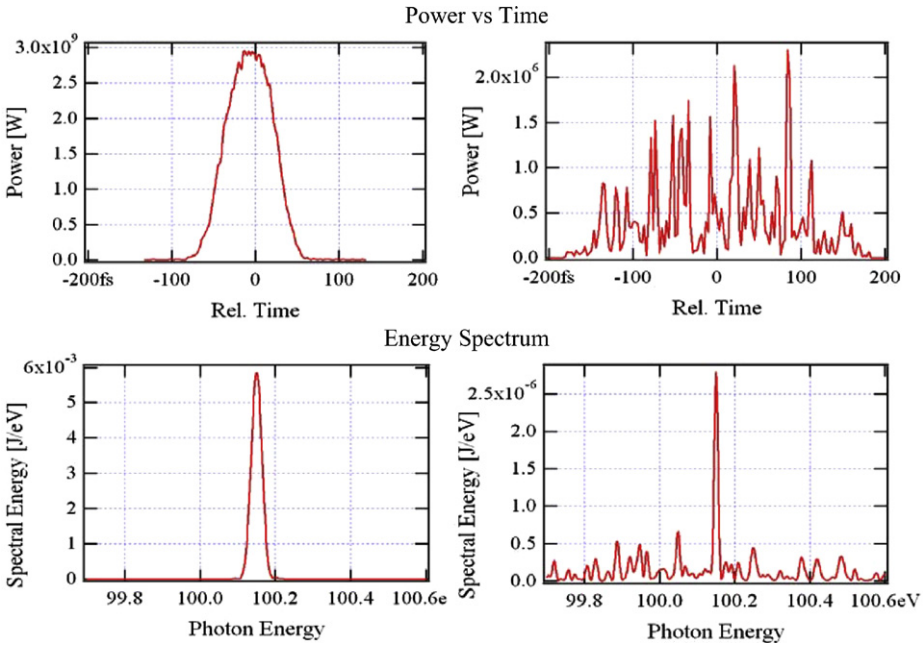

Fig. 1. Radiation characteristics at FEL exit for two cases: seeded (left) and started up from noise (right).

Electric field transformation at propagation from a transverse plane before an optical element (e.g., lens, mirror, aperture, zone plate, grating, …) to a plane immediately after it can be formally represented in frequency domain as

$$\vec{\tilde{E}}_{\perp \mathrm{out}}(x_2, y_2, \omega) \approx \mathbf{G}(x_2, y_2, \omega)\, \exp\left[\mathrm{i}\omega L x_2, y_2/c\right] \times \vec{\tilde{E}}_{\perp \mathrm{in}}(x_1(x_2, y_2), y_1(x_2, y_2), \omega) \quad (3)$$

where $\mathbf{G}(x_2,\ y_2,\ \omega)$ is a 2×2 matrix function of the output transverse coordinates and frequency, which can take into account eventual anisotropy of an optical element with respect to transverse components of the input electric field. The optical path function $L(x_2,\ y_2)$ and the input/output coordinate transformation $x_1(x_2,\ y_2)$, $y_1(x_2,\ y_2)$ can be found using the stationary

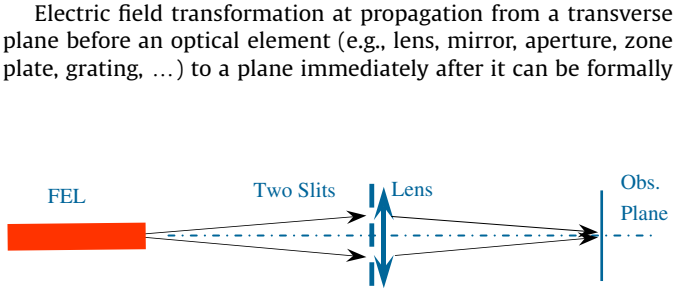

Fig. 2. Double-slit interferometer scheme.

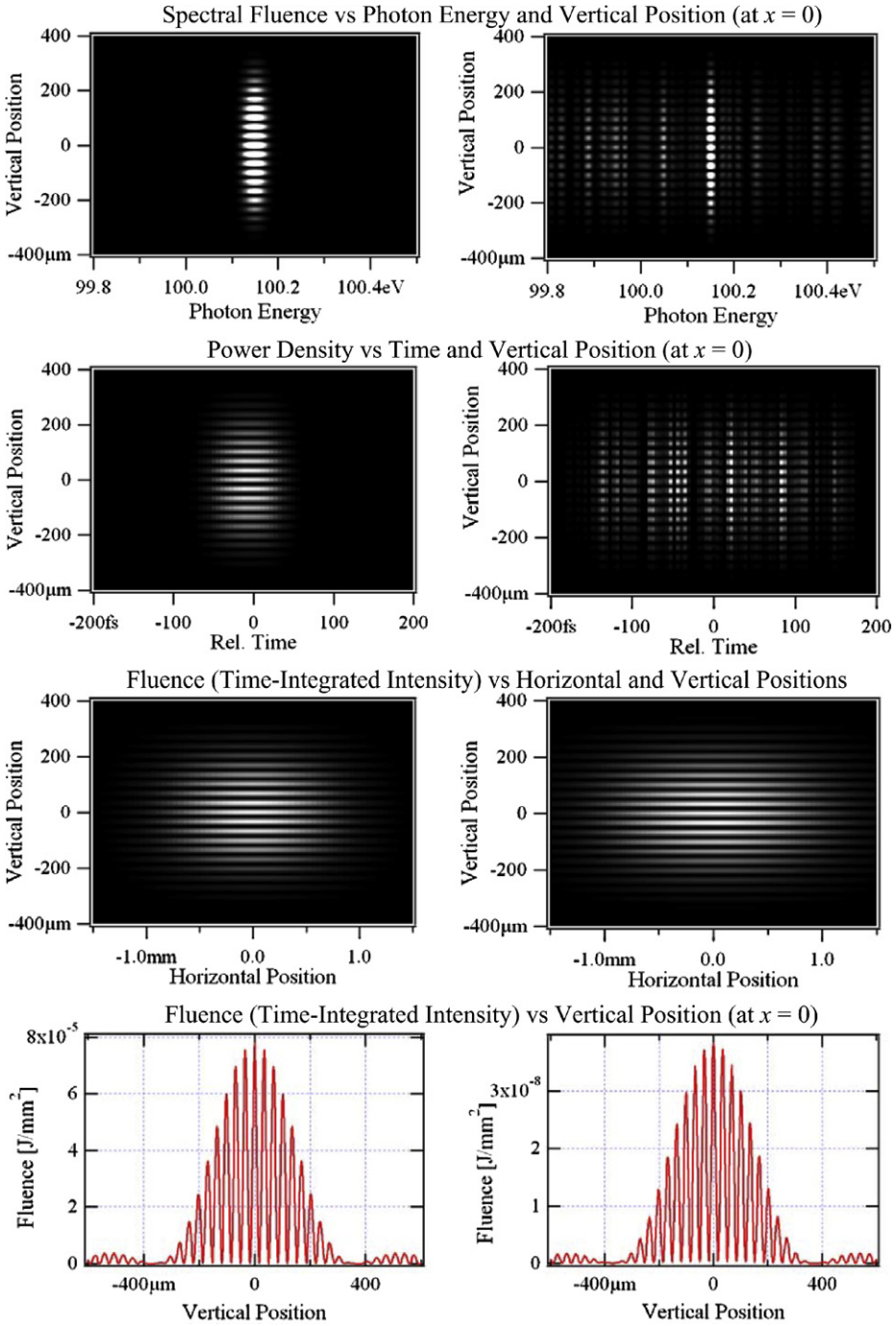

Fig. 3. Wavefront characteristics in observation plane of double-slit interferometer scheme for two FEL regimes: seeded (left) and started up from noise (right).

phase method or from geometrical optics (diffraction effects are neglected within L).

The simulation of wavefront propagation through a beamline consists in applying to electric field components repetitively the propagators described by Eqs. (2) and (3). Time-domain characteristics can be considered where necessary after applying Eq. (1). For some optical elements (e.g. for grating) time-domain propagator representations are numerically-efficient and can therefore be used in place of Eq. (3).

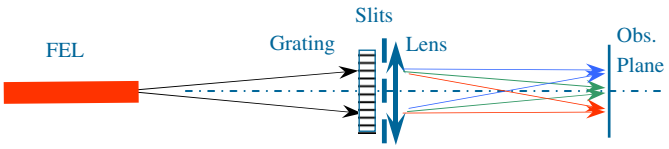

Fig. 4. Double-slit interferometer with grating.

3. FEL wavefront propagation examples

Two simple interferometer-type optical schemes are used in the examples below: one sensitive to spatial and the other to temporal coherence of input radiation. Two different time-dependent wavefronts are propagated and analyzed in the final observation planes: a wavefront obtained at seeded FEL operation and an unsaturated SASE wavefront.

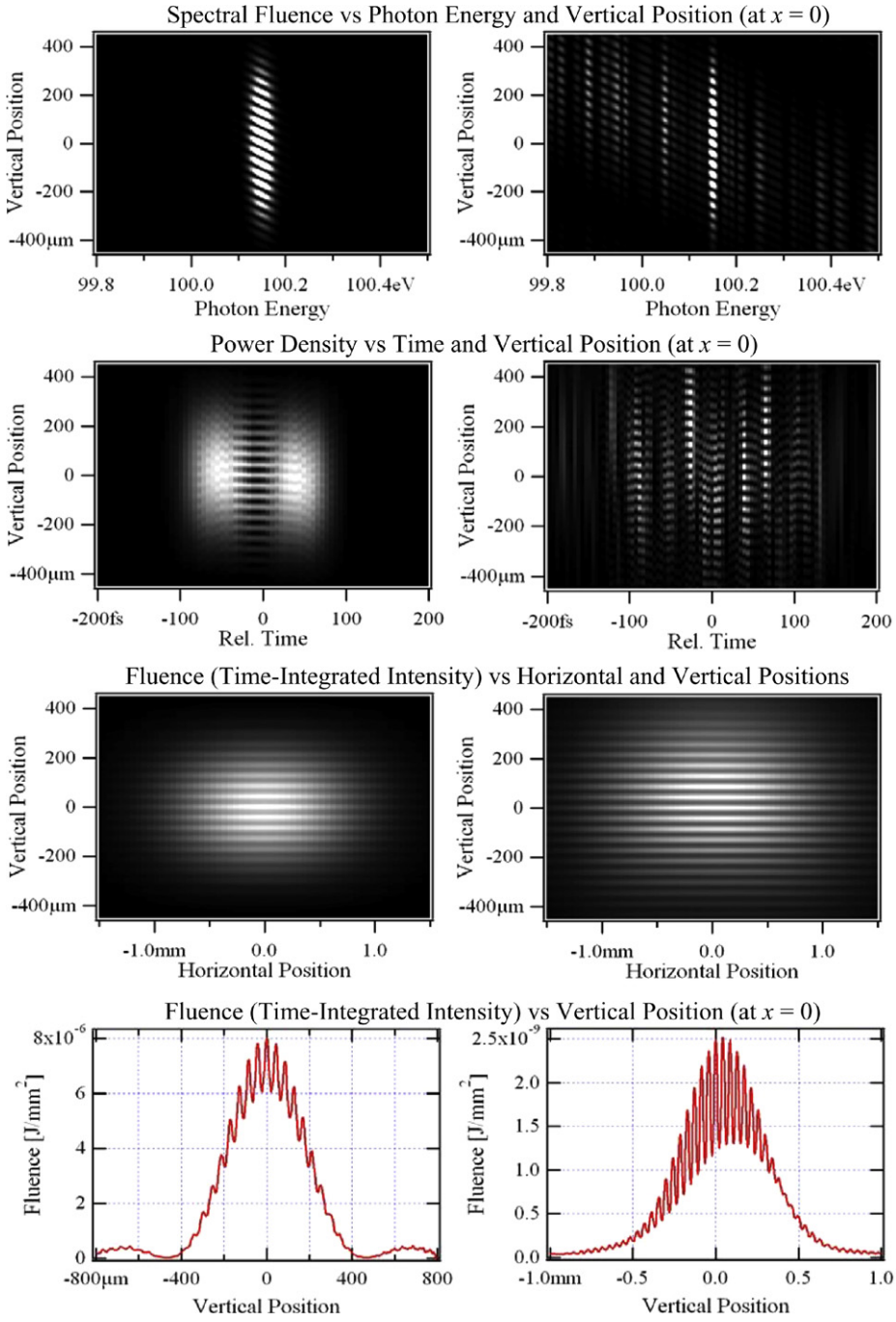

Fig. 5. Wavefront characteristics in observation plane of double-slit interferometer with grating, for two FEL regimes: seeded (left) and started up from noise (right).

All calculations described below were performed on a regular PC with only 1 GB of memory. Each wavefront propagation simulation took several minutes of CPU time, which is much less than the time used for calculation of the initial wavefronts.

3.1. Wavefronts at FEL exit

The two initial wavefronts were calculated using GENESIS for the parameters of the ArcEnCiel phase 2 project [17]: electron beam at 1 GeV energy, 1.5 kA peak current, 60 μm RMS bunch length, 1.2 π mm-mrad normalized emittance; planar undulator with 30-mm period and deflection parameter ~2, composed out of five 2-m long sections. In one case, a 50-kW peak power, 22-fs RMS duration 100.15-eV photon energy seeding radiation pulse was applied. In the other case, no external seed was used. Calculation results for the two cases are presented in Fig. 1.

3.2. Young's double-slit interferometer

Young's double-slit interferometer scheme (see Fig. 2) allows one to test spatial coherence of input radiation [16].

The following parameters of this scheme were used: 20-m distance from the FEL exit to the slits, 1-mm vertical space between the slits, 0.1-mm slit widths, 2.6-m/18-m vertical/horizontal focal distance of an astigmatic lens (mirror) and 3-m distance from the lens to the observation plane. The calculation results for the two wavefront cases (as described above) are presented in Fig. 3. One can see that in both cases, the visibility of interference fringes, characterizing the degree of spatial coherence, is ~1.

This result is in agreement with previous theoretical [12] and experimental data [14], suggesting relatively good transverse coherence of FEL radiation even in unseeded SASE case (before or at saturation).

3.3. Double-slit interferometer with grating

A simple optical scheme for probing temporal coherence can be obtained by inserting a grating into the double-slit interferometer, before (or after) the slits and the mirror, as shown in Fig. 4.

Wavefront propagation results for the two cases of input FEL radiation are illustrated in Fig. 5. At this calculation, the vertical and horizontal focal distances of the mirror were 3.7 and 100 m; the observation plane was at ~3.8 m from the mirror. The grating was assumed to be flat, with groove density of 150 l/mm; the incidence angle ~2.5° (in vertical plane).

We see from Fig. 5 that in both wavefront cases, the interference patterns are strongly modified by the grating. Vertical positions of interference peaks depend now on photon energy (upper image plots), and this reduces the visibility of fringes in the resulting frequency- (or time-) integrated patterns.

The poor visibility of fringes in the seeded case has simple time-domain interpretation: because of time delay introduced by the grating, the radiation pulses from the two slits almost do not overlap in time (see second image plot on the left in Fig. 5). This is a "signature" of typical "Fourier-limited behavior" of ultra-short pulses.

On the other hand, the reduced visibility of fringes in the SASE case is generally a consequence of spiky structure of the radiation pulse (second image plot on the right in Fig. 5). We note that the interference pattern obtained for this type of wavefront may appear further "smoothed-out" after averaging over ensemble of pulses (same applies to Young's scheme without grating discussed in Section 3.2).

4. Conclusions

Combining time-dependent FEL and Fourier optics based wavefront propagation simulations is completely feasible and offers clear benefits for FEL developers and users:

- these simulations provide radiation characteristics directly measurable in user experiments, eventually taking into account peculiarities of optics and detection schemes; this is very useful for fine-tuning of both the FEL and the optical beamline parameters for the needs of users;
- wave-optics phenomena occurring both in the processes of generation and in the propagation of time-dependent FEL wavefronts (diffraction, pulse lengthening, …) can be effectively simulated in one computational framework (involving FFTs); this is particularly convenient for simulation of pulses that are close to diffraction- and Fourier limits.

Acknowledgments

We would like to thank Luca Giannessi (ENEA Frascati) for fruitful discussions and encouragement to develop software functions for efficient time-dependent FEL wavefront propagation simulations.

This work was supported by EU Commission in the Sixth Framework Program, Contract no. 011935-EUROFEL.

References

[1] C. Pellegrini, S. Reiche, Optics Encyclopedia, Wiley-VCH, Berlin, 2003.
[2] A. Zholents, W. Fawley, Phys. Rev. Lett. 92 (2004) 224801.
[3] K.-J. Kim, Nucl. Instr. and Meth. A 246 (1986) 71.
[4] J. Bahrdt, Appl. Opt. 36 (19) (1997) 4367.
[5] J. Bahrdt, Phys. Rev. Spec. Top.—Accel. Beams 10 (2007) 060701.
[6] J.W. Goodman, Introduction to Fourier Optics, second ed., McGraw-Hill, New York, 1996.
[7] O. Chubar, P. Elleaume, in: Proceedings of EPAC-98, 1998, p. 1177.
[8] O. Chubar, et al., Proc. SPIE 4143 (2000) 48;
O. Chubar, et al., Proc. SPIE 4769 (2002) 145.
[9] P. van der Slot, in: Proceedings of FEL-2007, 2007, p. 207.
[10] S. Reiche, 〈http://corona.physics.ucla.edu/~reiche/〉.
[11] R. Tatchyn, J. Arthur, Proc. SPIE 3451 (1998) 193.
[12] E. Saldin, E. Schneidmiller, M. Yurkov, Nucl. Instr. and Meth. A 507 (2003) 106.
[13] Y. Li, et al., in: Proceedings of PAC-2003, 2003, p. 905.
[14] R. Ischebeck, et al., in: Proceedings of EPAC-2004, 2004, p. 2581.
[15] T. Watanabe, et al., Phys. Rev. Lett. 98 (2007) 034802.
[16] M. Born, E. Wolf, Principles of Optics, Pergamon Press, Oxford, 1970.
[17] M.-E. Couprie et al., in: Proceedings of FEL-2007, 2007, p. 505.